ISSN 1349-1113
JAXA-RR-04-005E

JAXA Research and Development Report

X-Band Deep Space Digital Transponder and Regenerative Ranging

Tomoaki TODA, Hirofumi SAITO, Zen-ichi YAMAMOTO,
Hideho TOMITA, Kazumi SAGAWA, Shinji YAMADA,
and Kazutoshi SUGIYAMA

October 2004

Japan Aerospace Exploration Agency

X-Band Deep Space Digital Transponder and Regenerative Ranging

By

Tomoaki Toda[1], Hirofumi Saito[1], Zen-ichi Yamamoto[1], Hideho Tomita[1], Kazumi Sagawa[2], Shinji Yamada[2], and Kazutoshi Sugiyama[2]

Abstract : The improvement of X-band deep space communication capability has strongly been demanded to enhance planetary exploration activities at Institute of Space and Astronautical Science (ISAS). This paper presents our newly developed X-band transponder meeting requirements imposed by future ISAS deep space missions. Some particular technologies adopted in it are also explained in detail to show how the transponder was optimized under the restricted condition in ISAS. Among them are digital signal processing in demodulator, frequency scheme enhancing the use of commercially-off-the-Shelf (COTS) products, and employment of simplified regenerative ranging. Above all the new properties of our transponder were successfully verified using its engineering model (EM) developed for functional testing. Particularly, the new regenerative ranging scheme implemented in our transponder was proved to be competitive with regenerative ranging of Jet Propulsion Laboratory (JPL) while achieving its drastic cost saving in the development process. The transponder is now ready for the development of prototype model (PM).

Key words : deep space, digital transponder, X-band, regenerative ranging

1. Introduction

The reliability is one of the most requisite conditions of onboard communication systems. In such a system, only well-established technologies are permissible to be applied for innovation. However, it has recently been understood that a small conservative change is insufficient for supporting more complicated deep space missions. The development of a new deep space transponder is now considered as one of the key technologies in Institute of Space and Astronautical Science (ISAS).

Table 1 summarizes X-band deep space transponders of National Aeronautics and Space Administration (NASA), European Space Agency (ESA), and ISAS. These are based on the papers available for authors [1-5]. Though it is difficult to discuss transponder's superiority simply by these skin-deep data, NASA/JPL's transponder looks outstanding in mass and power consumption considering that it also covers Ka-band communication. Their transponder is built of collected application specific integrated circuits (ASICs) and monolithic microwave integrated

[1] Institute of Space and Astronautical Science/Japan Aerospace Exploration Agency, 3-1-1, Yoshinodai, Sagamihara, Japan, 229-8510, Japan

[2] NEC/TOSHIBA Space Systems Ltd/4035 Ikebe-cho, Tsuzuki-ku, Yokohama, Kanagawa, 224-8555 Japan
Phone: +81-42-759-8343 Email: toda@pub.isas.jaxa.jp

circuits (MMICs). Most of them are a custom component specially designed for their transponder, which effectively contributes to the total miniaturization. But we have to find our own solution in the way suitable to our permissible budgetary condition. The report presented in the following sections is our answer to this question. To output competitive results at lower cost.

Table 1 Comparison of X-band deep space transponders.

	NASA/JPL *1	NASA/APL	NASA/APL *2	ESA *3	ISAS *7
Volume [cm^3]	N/A	10x10x6	N/A	25.4x18.5x16 *5	19x16x10.3(Rx) 16.8x14.3x9(Tx)
Mass	3.0 kg	1.0 kg	1.32 kg *5	6.5 kg	3.76 kg
Power Consumption	12.9 W *4	11.7 W *4	12 W	22 W*6	28 W
Carrier Acquisition Threshold	-157.4 dBm	-162 dBm	-155 dBm	-152 dBm	-144 dBm
Spacecraft	DS1	Not completed	CONTOUR	ROSETTA, Mars Express	HAYABUSA
Reference	[1]	[2]	[3]	[4]	[5]

*1 National Aeronautics and Space Administration/Jet Propulsion Laboratory (NASA/JPL).

*2 Johns Hopkins University/Applied Physics Laboratory (APL).

*3 European Space Agency (ESA).

*4 JPL's transponders provide a Ka-band communication capability. But their power consumption is given with its function turned off.

*5 APL's unit is composed of 2 card modules of uplink and downlink. Hence housing material contribution is not considered in its mass estimation.

*6 ESA's transponder contains both S-band and X-band communication capability. The power consumption is given with its S-band transmitter turned off.

*7 ISAS's transponder is composed of independent receiver (Rx) and transmitter (Tx) boxes. Rx has an incomplete redundant configuration. Therefore, the mass and power consumption are estimated based on its equivalent model.

2. Requirements for a new transponder

General requirements for a new transponder are as follows. Its production cost must meet a demand of our current and future science projects. It should be smaller in size, mass and power consumption without sacrificing its performance. The compatibility with our established ground communication systems is necessary. It is also desirable to be compatible with oversea station equipments in order to have their support of tracking and data acquisition. And finally a new transponder has to be designed so that it responds to as many requests expected by our future missions as possible. Satisfying these issues, the new properties given to our transponder were defined as below.

- Digital signal processing in demodulator.
- Frequency synthesis suitable for the use of commercially-off-the-shelf (COTS) products.
- Onboard implementation of regenerative ranging capability.

In the following paragraphs, we explain briefly what meanings they have in our new transponder.

2. 1. Digital signal processing in demodulator

The demodulator of our previous transponder has been traditionally made of analog circuits. However, radiation tolerant programmable devices are now ready to use for digital processing in space instruments. Though it has long been difficult to replace analog circuits with corresponding digital ones in ISAS due to a very limited development time and cost, we now at last have a chance to do so. The introduced digital processing helps us to save cost and time needed for a complicated adjustment of microwave analog circuits. It is also expected to contribute to an improvement of receiver sensitivity and performance stability. The linearity in setting parameters in digital processing gives us a very simple way to control our transponder. The flexibility in circuit design is important, too. Needless to say, that enables us to modify transponder properties at any phase of development. Thus, we decided to apply digital signal processing to the demodulator unit in our transponder. This unit covers the whole process starting from received intermediate frequency (IF) signals.

2. 2. Frequency synthesis for the use of COTS products

The effective way to suppress the cost of space-use instruments is to enhance the number of COTS devices used in it. But it has been difficult due to the lack of useful database and shortness of development time. As a solution to this difficulty, frequency relationships in the synthesizer of our transponder were designed so that it enables us to choose as many COTS products as possible from the COTS list we have. The idea to develop ASICs or MMICs in our transponder was not taken from the first in this project. Though their use is obviously the most attractive way to miniaturize a transponder beyond the limit of available space-use discrete devices (see Table 1), its investment was not balanced with the cost for our future transponder.

2. 3. Incorporation of regenerative ranging

The regenerative ranging improves a ranging link capability between spacecraft and ground stations [6]. In our deep space missions, gimbals for pointing onboard high gain antenna (HGA) at a ground station are likely to be omitted mainly due to the launch mass limit of space vehicle, M-V rocket. Therefore, the communication and ranging link must be established with onboard medium gain antennas (MGAs) in our nominal operation, including emergency cases of spacecraft. The bottleneck in the above link is understood to be the ranging link because the ranging signal quality is degraded through both propagation of uplink and downlink. Figure 1 is an example of our ranging capability to reveal this difficulty. The calculation assumes the use of onboard MGA of 16 dBi and the ø64 m antenna at Usuda

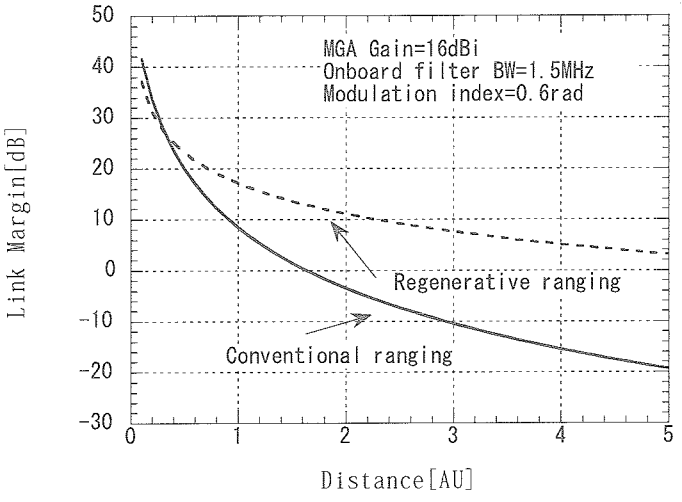

Fig.1 Deep space ranging capability in ISAS assuming the use of an onboard MGA of 16 dBi and UDSC-64.

Deep Space Center (UDSC-64). It indicates that the conventional turn-around ranging is possible at most within 1.6 AU (astronomical unit). This restricted distance becomes even shorter when only a smaller aperture antenna of our ground facility is available due to contingency. Figure 1 shows that the regenerative ranging is effective to overcome this situation. The ranging link over 5 AU is possible with regenerative ranging. And the obtained extra margin in ranging link increases operational reliability because the ø34 m antenna station in Uchi-no-ura Space Center (USC-34) could be a backup of the 64 m one. According to Figure 1, USC-34 is available for ranging operation approximately within the area of 4 AU provided that the new power amplifier (5kW output) is installed in USC-34.

3. X-band transponder

We have developed EM of X-band transponder (Figure 2). The transponder is composed of 4 units: from above, respectively, digital signal processing unit (DSP), radio frequency unit (RF), frequency synthesizing unit (FS), and power supply unit (PS). The inside of each unit is displayed in Figure 3. They were integrated in such a manner that they could be PM of transponder by replacing their critical commercial parts with equivalent qualified products. We will discuss more on it in the section 4. The non-flight commercial parts in EM were used to suppress the development cost.

3. 1. Properties of EM transponder

The size of EM was 15 cm in width, 15 cm in depth, and 9.5 cm in height. The weight and power consumption were 3.4 kg and 19.8 W respectively. The frame is made of Al to economize the cost of EM. The given power consumption does not contain an oven controlled crystal oscillator (OCXO) contribution. The OCXO is placed outside of EM. But it will be located inside of PM to be constructed. According to our latest estimation for PM, the weight and power consumption will be improved to be 2.1 kg using Mg as housing material and 18.2 W with a transient OCXO operation included. The properties of our EM transponder are summarized in Table 1. Its acquisition threshold was designed to be lower than -150 dBm. The measured noise figure at the receiver input was 1.53 dB. As other specifications, the variable modulation index with a step of 0.01 rad up to1.4 rad and the selectable discrete command bit rate are to be mentioned.

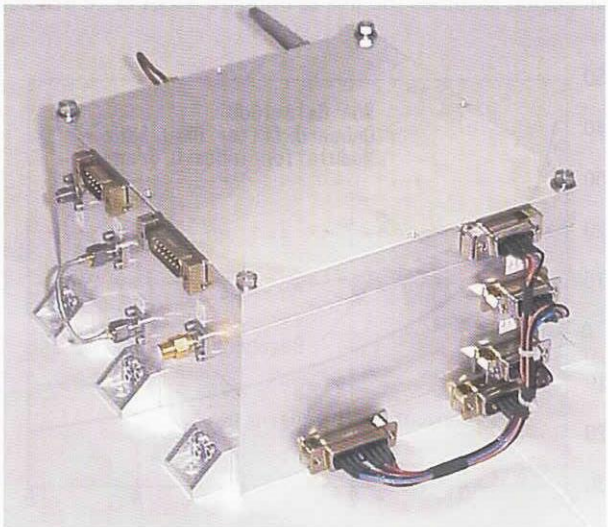

Fig.2 Engineering model of digital X-band transponder: 15 cm in width, 15 cm in depth, and 9.5 cm in height.

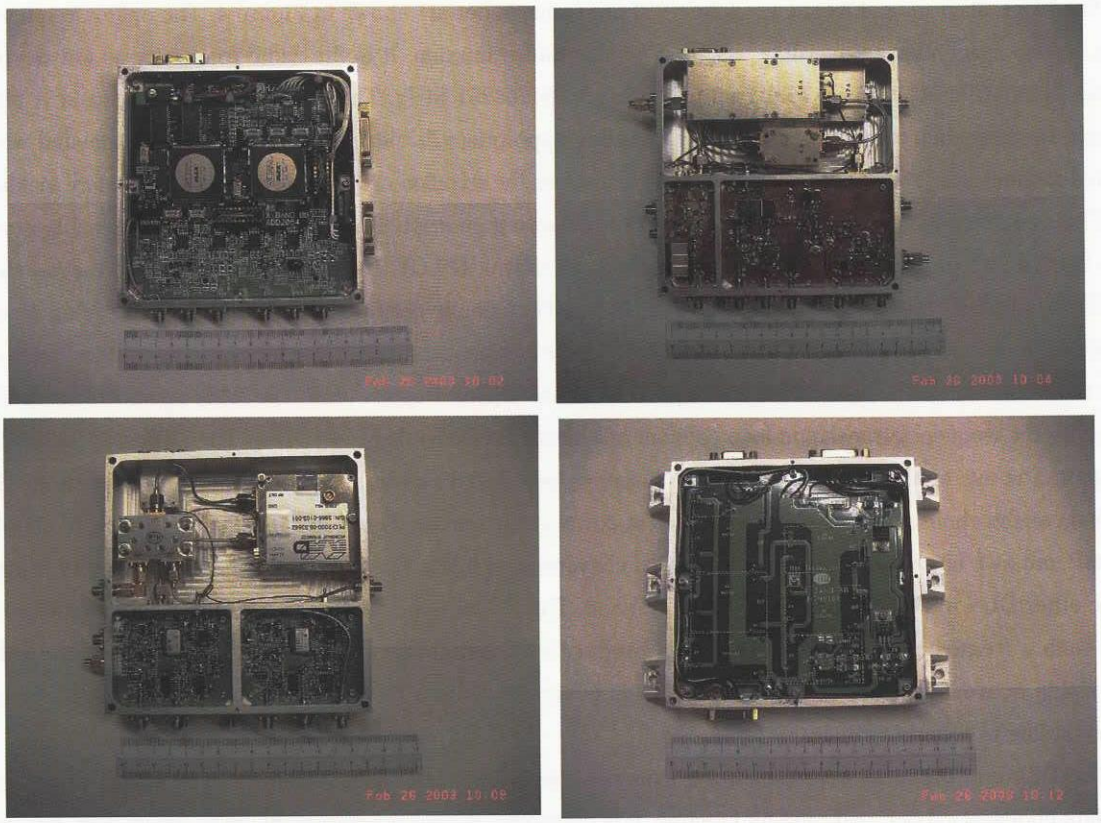

Fig.3 Units of X-band digital transponder. Left up: DSP unit, right up: RF unit, left down: FS unit, and right down: PS unit.

Table 2 Properties of digital X-band transponder.

Parameter	Nominal value
Frequency (Uplink/Downlink)	7156.23MHz/8408.21MHz
Noise figure	1.53dB
Carrier acquisition threshold	<-150dBm
Tracking signal range	-150dBm~-70dBm
Tracking frequency range	±100kHz
Output level	20dBm
Mass	3.4kg
Power Consumption	19.8W
Volume	15*15*9.5cm^3

3. 2. Transponder design

The block diagram and frequency scheme of our transponder are shown in Figure 4. The uplink frequency was set at a deep space channel possibly assigned for our future mission. It is the same frequency as our deep space mission "HAYABUSA", that is, $749F_0$ with F_0 being 9.554783951 MHz. The coherent frequency ratio is 880/749. Though the frequency channel is variable by choosing appropriate F_0, filter parameters must be adjusted when the selected channel is far away from the above one. In that sense, the selection of F_0 should be confirmed before making PM.

The frequency loop was designed based on the following concept. The 1st local frequency signal is generated from the OCXO output through a phase locked oscillator (PLO). Its frequency was selected so that the downlink/uplink 1st IF frequency ratio was nearly 2:1. This simple relationship makes the succeeding frequency synthesis simple and contributes to the reduction of device components used in the system. The 2nd local frequency is made of $248.5F_0$ and the offset of $0.25F_0$+fd, where fd denotes uplink Doppler shift. The latter uplink coherent signal is formed by the frequency translation loop containing a direct digital synthesizer (DDS). The DDS is embedded in the DSP unit. The use of DDS in the frequency translation loop enables us to handle a lower input frequency, which is advantageous to choose COTS products with a less power consumption. The gain controlled 2nd uplink IF is passed to the DSP unit as 8 bits digitized data after the final conversion to $0.5F_0$. The downlink coherent frequency is prepared by the other DDS in DSP unit as $0.5F_0+(880/749)\times$fd. The 2nd term is a Doppler shift multiplied by coherent ratio. Even such a frequency relationship is simply produced by digital signal processing. In Figure 4, the coherent relationship between uplink and downlink carrier is generated in each DDS simply by the multiplication of number corresponding to coherent ratio.

The DSP unit performs demodulation of command signal, accumulation of gain control signal, regeneration of downlink coherent carrier, and ranging function. It is composed of field programmable gate arrays (FPGAs), random access memory (RAM), read-only memory (ROM) to initialize FPGAs, and interfaces to other units. The new regenerative ranging is equipped in this DSP unit. It is programmed together with conventional turn-around ranging and either ranging is selected by a command sent to spacecraft. The new ranging is discussed in detail in the section 5.

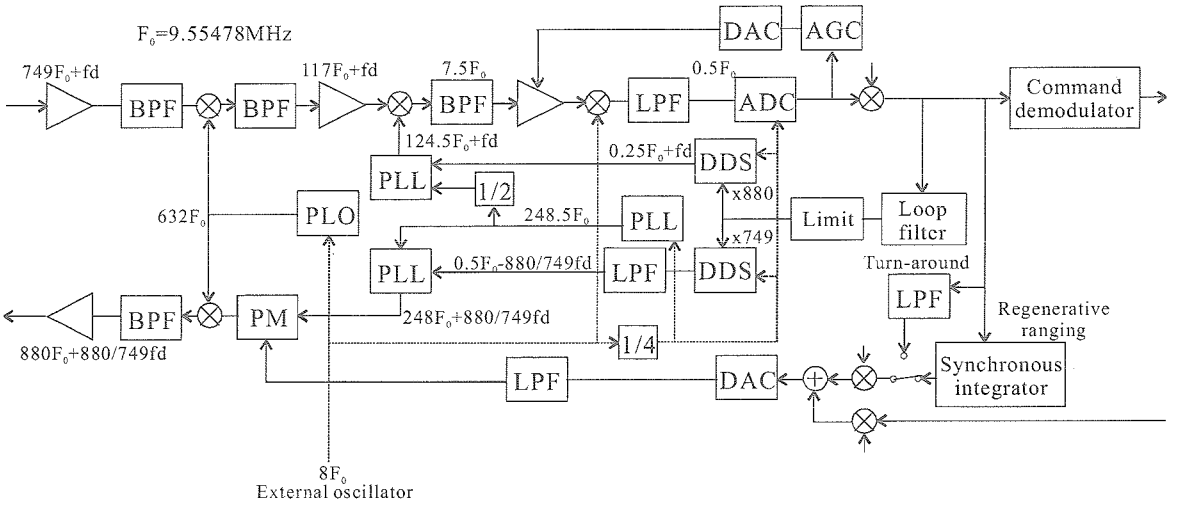

Fig.4 Block diagram and frequency relationship of digital X-band transponder.

The functional testing of EM transponder was carried out successfully. The generated coherent downlink carrier was stable. The relative frequency deviation of returned carrier was lower than 5×10^{-12} with the input signal level more than −150 dBm. And Figure 5 is the result of command bit error rate measurement.

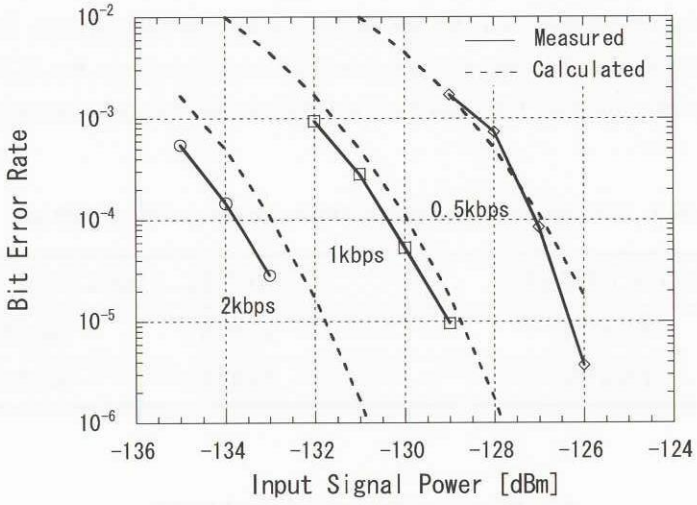

Fig.5 Command bit error rate of digital X-band transponder. Sinusoidal subcarrier was used with modulation index of 0.1 rad. Due to the error of 1dB to estimate the net input signal power, the measured BER looks better than the ideal one.

4. Assessment for flight qualification

The EM transponder has been designed considering a roadmap to its flight model. For instance, some radio frequency devices are to be packaged in a module to keep size reduction of EM in PM. Figure 6 shows such a multi-chip module (MCM) developed as an X-band low noise amplifier (Gain=35dB, NF=1.2dB, 80mA/5V). It is composed of a high electron mobility transistor (HEMT) and a space-use commercial MMIC with an amplifier and an isolator in it. The availability of selected COTS devices was also an important issue because it is uncertain for most of them whether to be supplied even after 10 years. In our transponder, they are selected so as to be obtainable or substitutive at least in the next 10 years.

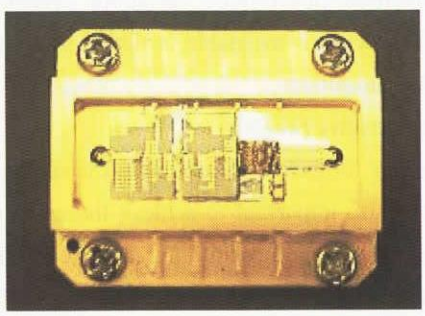

Fig.6 Hybrid chip module of low noise amplifier developed for digital X-band transponder.

The biggest issue to upgrade our transponder from EM to PM was a transfer of hardware definition language (HDL) program of FPGAs to that of radiation tolerant products. We used ALTERA FLEX10K100 in EM. 2 FPGAs were employed to accommodate all the necessary transponder functions related with command, telemetry, and

ranging in DSP unit. And then we will take another two steps to develop this unit of proto-flight model. The preliminary HDL program for ALTERA devices are moved to a commercial ACTEL A54SX72S in PM and then to RadHard FPGAs, ACTEL RT54SX72S of PFM.

The DSP unit of PM has recently been developed following the evaluation of EM. Through its verification test, the equivalency of HDL program between ALTERA and ACTEL device was fully checked. Table 3 shows how many percent of cells in FPGA are used in the DSP unit and how different it is between the ALTERA (EM) and ACTEL (PM) device. Since there is still more than 15% unused cell in FPGA, further functional optimization in DSP unit in PM is possible.

Table 3 Comparison of used cells in FPGAs for EM and PM of DSP unit.

ALTERA FLEX10K100 for EM			ACTEL A54SX72S for PM	
FPGA1	85.50%	⇒	FPGA1	88.22%
FPGA2	69.47%	⇒	FPGA2	63.15%

5. Regenerative ranging of ISAS

In a deep space mission, the conventional turn-around ranging signal is severely degraded through its propagation. In this scheme, the noisy signal received by a spacecraft is simply passed through an onboard low-pass filter after carrier demodulation. Then, it is amplified, modulated onto a downlink carrier, and retransmitted to a ground station. But this amplification is rather dissipative because its input signal is very noisy and the ranging signal is embedded in it. The regenerative ranging is an effective way to minimize this loss. We have already shown how it works for spacecraft of ISAS in the section 2.

The onboard regeneration of received signal is an established technology. It would be easy to find documents on it. But it had not been applied to ranging signal of spacecraft until JPL adopted it in its new transponder [2]. One reason is the latency to introduce digital signal processing in deep space technologies. The unknown additional phase delay variation by regeneration process may severely degrade range accuracy. That is never permissible in deep space exploration. Especially when ranging plays an important role in scientific observations, there is no compromise in its accuracy in science. Such inconvenient phase delay variations possibly caused by environmental or aging influences during the long journey of spacecraft is avoidable in digital signal processing. Therefore, it is natural to introduce regenerative ranging in digital transponder.

5. 1. Synchronous integration for regenerative ranging

Our interest is in confirming whether the range measurement is really possible without degradation by the introduced signal regeneration. And it is also important to achieve the same measurement quality as conventional turn-around ranging in the simplest manner. We propose a different regenerative ranging scheme from JPL. It is an onboard synchronous integration for the combined PN code ranging signal: PN511∩PN255, where PN511 and PN255 denote the PN code with symbol length of 511 and 255 respectively. The synchronous integration is equivalent with filtering by weighted addition over the long periodical code. Therefore, there is no difficulty in its implementation for a new transponder. And above long, but simple combined code is compatible with our near-earth ranging equipment in USC and UDSC [7]. Only a slight modification of ground ranging equipment is sufficient when applied to deep space ranging. The proposed scheme is superior to JPL's method in its simplicity and flexibility. JPL scheme requires a

high-speed onboard correlator specific to their original ranging code together with the counterpart of ground facility. When one applies JPL scheme to their spacecraft, he encounters both costly development of onboard and ground facility correlators. However, our scheme basically demands only the periodicity of ranging codes and thus, enables other users to customize it and make the best use of their established ranging facility when they needs regenerative ranging.

Though the above ranging code is selected from the viewpoint of compatibility with our ground facility, we can say that it is suitable to our proposed scheme for their balanced signal power distribution to PN511, PN255, and clock component. For example, JPL's regenerative ranging code is given as modulo 2 addition of PN sequences of lengths, 2, 7, 11, 15, 19, and 23 [*6*]. It gives most power to a clock component, that is, PN code of length 2 than the other PN codes. If we use such a code in our scheme, it takes much longer time to integrate all the component codes to the quality of regeneration. Therefore, the PN codes of fewer components but a length enough to resolve range ambiguity are recommended for our regeneration scheme.

Our regeneration process was achieved with the simple circuit shown in Figure 7. The degraded signal to noise ratio (S/N) of each PN component is recovered by the repetitive addition of corresponding signals in this circuit. The each integrated result memorized in RAM is recalled for another summation every time the corresponding symbol in the periodical signal is received. The regeneration process is terminated when the quality of ranging signal becomes good enough to make hard-decisions. This termination is determined by the leakage coefficient α in Figure 7. The signal interpreted as a discrete value is finally modulated onto downlink carrier. This is all for the onboard regeneration circuit.

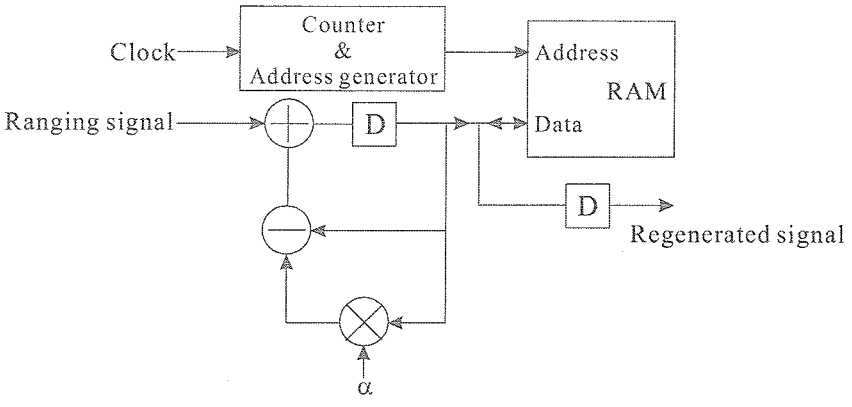

Fig.7 Synchronous integration circuit for regenerative ranging.

The integration time is an important parameter to evaluate our proposed scheme. This parameter is determined by permissible number of bit errors caused by hard-decision process in regeneration. In fact, we have to discuss here the quality difference between our proposal and JPL's method. Our regeneration scheme should precisely be called quasi-regeneration because it does not give us any information on the sequence of PN codes. And it is impossible to correct an error in received data. It simply works for refining the quality of ranging signal. Therefore, we cannot avoid bit errors in the sequence of ranging signal introduced by the hard-decision process. And this leads to the power loss of ranging link. On the contrary, the bit errors are supposed to be corrected in JPL scheme thanks to the complete regeneration by onboard correlators. From this point, our method inevitably needs a longer integration time for regeneration against severely degraded uplink signals.

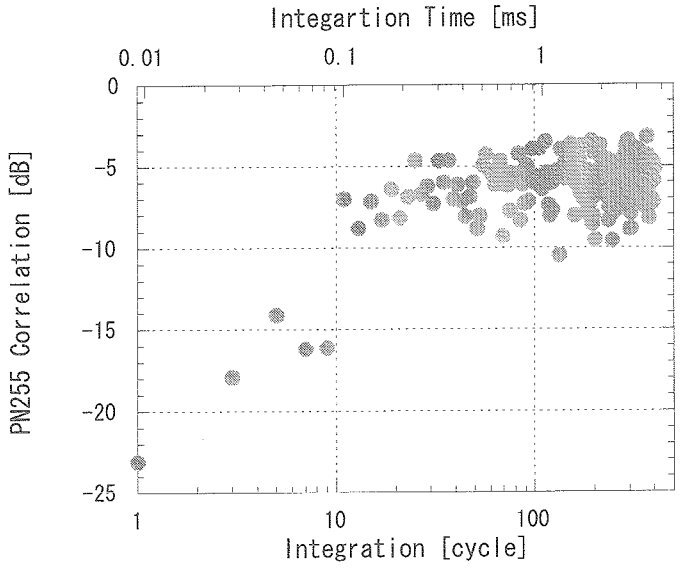

Fig.8 Estimated onboard integration time needed for PN255 regeneration under the condition of HAYABUSA.

Figure 8 shows how many times of integration are needed for the case of HAYABUSA, where the received signal energy per chip to noise density is less than -10dB. This is approximately the case where spacecraft of ISAS are distant from the earth by 2 AU. The vertical axis is a normalized power of correlation between regenerated ranging signal and PN255 sequence. The horizontal axis is onboard integration number or integration time. The regenerated PN255 signal quality is converged after around 1 ms of integration although more integration is necessary to suppress

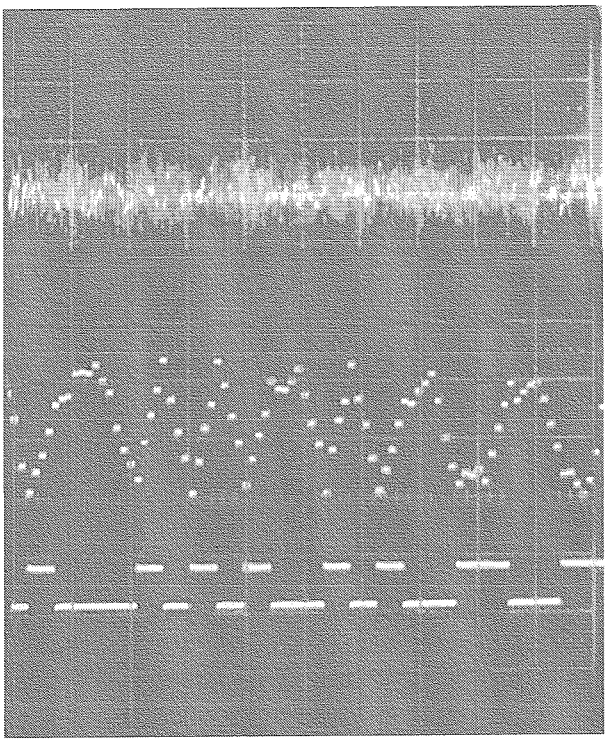

Fig.9 Improved ranging signal quality by synchronous integration. High: conventional, middle: regenerative, and low: original ranging signal. The horizontal axis is 20μs/DIV. The vertical axis is scaled to each signal level.

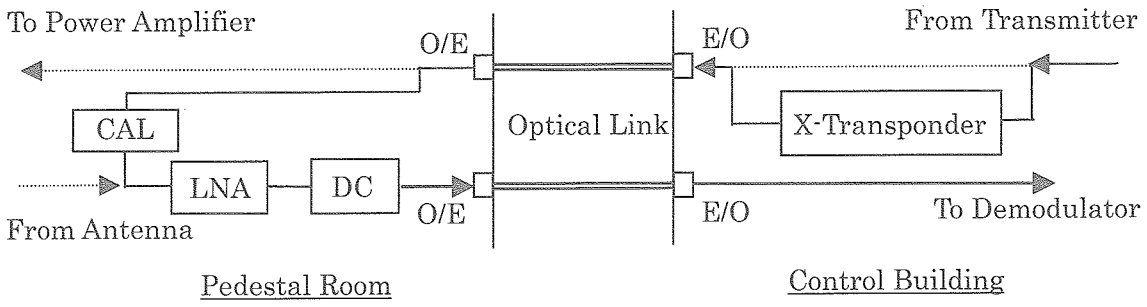

Fig.10 Compatibility test configuration in UDSC.

its fluctuation. Since another 10dB improvement is sufficient for that purpose, the integration time is at most 100 ms. PN511 signal needs twice integration time of PN255. Thus, the required integration time is approximately less than 1 s for our latest deep space mission. It is obviously small and negligible comparing with the propagation delay time between spacecraft and the earth. Hence, we can conclude that the lack of error correction does not bring us any difficulties on the spacecraft operation. Note that the estimated time here is just the integration time in the regeneration circuit. The total time exclusive of propagation delay needed to start ranging also depends on the onboard time constant needed for capturing carrier and subcarrier, that of ground receiver, and correlation process time of ground ranging system.

5. 2. Verification based on EM transponder

The effectiveness to use synchronous integration for the signal regeneration was examined by using the EM transponder in section 3. The comparison between our conventional turn-around ranging and regenerative ranging is presented in Figure 9. They are eye patterns of PN255 signal to be modulated onto a downlink carrier. The received signal power of transponder was lower than -145 dBm and the modulation index of ranging signal was 0.8 rad for both cases. The chip rate of ranging signal was around 109.2 kcps. The square pattern on the lower side in Figure 9 is a reference PN255 ranging signal. The pattern on the higher side corresponds to turn-around ranging. We can no more determine how the signal originally was from this output. However, the regenerated signal pattern in the middle shows a clear coincidence to the reference. Note that the sign of regenerated signal pattern is inverted in Figure 9. The regeneration of ranging signal by the synchronous integration was experimentally confirmed. The similar result was obtained for PN511, too.

The compatibility test of regenerative ranging with our ground facility was done. The EM transponder was combined with equipments in UDSC. The test configuration was built by closing a local loop in the ground station facility (Figure 10). The transponder was located in an air-conditioned room during the experiment. In this configuration, the range standard deviation was measured with the ground ranging equipment. The ranging mode was set for near-earth satellites instead of deep space mode because present deep space mode uses a different code sequence from that of regenerative ranging. It is due to this mode selection that tracking for conventional turn-around ranging signal is out of use below -130 dBm in Figure 11. The uplink power was fixed at -135 dBm which was the lowest uplink power keeping a stable coherent downlink carrier of transponder. Below this input level, the coherent downlink carrier frequency dispersion increases gradually as a result characterized by phase locked loop (PLL) of transponder. The modulation index was set at 0.7 rad for uplink and at $\pi/4$ rad for downlink. The received downlink power was varied as a parameter. The measured range values at the various downlink powers were almost kept at constant. Its variation was less than ± 1 m for both the conventional and regenerative ranging method. Figure 11 is

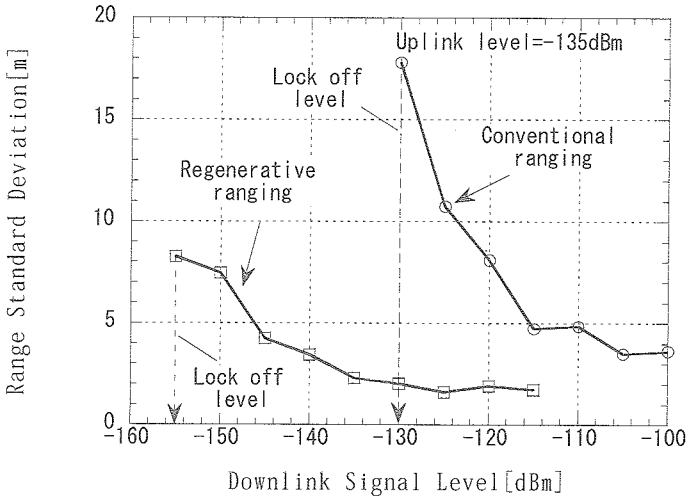

Fig.11 Ranging stability between conventional (turn-around) and regenerative ranging.

the variation of range deviation in the above experiment. The horizontal axis is the input downlink signal level to ground receiver. It shows that the regenerative ranging link is better than the turn-around ranging by more than 25 dB in the received downlink signal level. And the range dispersion is below 10 m even at -150 dBm downlink signal power. The floor level difference at the higher input power is due to the difference in equivalent filter bandwidth of conventional and regenerative ranging. The regenerative ranging has a narrower bandwidth resulted from the signal integration process. Around 4 dB improvement in Figure 11 is in accordance with an approximate 10 times integration in the regeneration process.

Finally, the temperature dependency of ranging function was evaluated. Digital signal processing was introduced for the first time in our transponder. Because deep space spacecraft sometimes experience a very stringent thermal environment, the temperature property of their communication system is very important. The experiment was carried out using PM of DSP unit introduced in section 4. The EM was developed for a functional demonstration of future transponder. However, as the PM of DSP unit was ready for this experiment, we made a decision to carry out this experiment by combining it with the rest of EM transponder. Only the DSP unit was placed inside an environmental chamber during the experiment. Thus, the temperature dependency of RF devices does not influence on this experiment. The phase difference between transmitted and returned ranging signal was evaluated in the temperature range of -30℃～60℃ while the uplink input power was varied in the range of -145 dBm～-70 dBm for regenerative ranging and -110 dBm～-70 dBm for turn-around ranging. The modulation index for uplink signal was 1.0 rad for the both ranging scheme. The averaged delay time of returned ranging signal was 28.16 μs and 3.35 μs for the regenerative and turn-around ranging respectively. This difference comes from the integration time of regeneration process. The peak-to-peak variation of delay time through the change of temperature and uplink input level was within 30 ns for the regenerative ranging and 20 ns for the conventional ranging. The degradation in raging quality at -145 dBm is minimized thanks to the regeneration effect.

6. Conclusion

We have developed a new X-band deep space transponder for future deep space explorations in ISAS/JAXA. The mass, size and power consumption were reduced in comparison with our previous X-band transponder. Digital

processing in demodulation and ranging, new frequency scheme to enhance the use of COTS products, and simplified regenerative ranging were newly employed. They all were examined and worked well in the EM of transponder. Especially, our original regenerative ranging showed an economic way to introduce a competitive ranging performance with that proposed by NASA/JPL. The assessment for flight qualification was also taken into account in the design of new transponder. It will help a prompt application of above new technologies to the PFM of our transponder.

References

[1] C.C. Chen, M. Herman, A. Makovsky, S. Shambayati, F.H. Taylor, S. Zingales, C. Nuckolls, and K. Sieman, "Small Deep Space Transponder (SDST) DS1 Technology Validation Report", JPL document.

[2] J.B. Berner, S. Kayalar, and J.D. Perret "The NASA Spacecraft Transponding Modem", Proc. IEEE Aerospace Conf. 2000, vol.7, pp.18-25, Mar. 2000.

[3] R.S. Bokulic, M.J. Reinhart, C.E. Willey, R.K. Stilwell, J.E. Penn, J.R. Norton, S. Cheng, D.J. DeCicco, R.C. Schulze, "Advances in deep-space telecommunications technology at the Applied Physics Laboratory", Acta Astronautica, vol.52, pp.467-474, 2003.

[4] M.C. Comparini, L. Simone, and G. Boscagli, "Deep Space Digital Transponder for Rosetta and Mars Express Mission", ESA Workshop on Tracking, Telemetry, and Command System for Space Applications, pp.169-176, 2001.

[5] T.Toda, Z.Yamamoto, H.Saito, H.Hirosawa, I.Nakatani, and H.Tomita, "Innovative Deep Space Small Transponder Equipped with Simple Regenerative Ranging", ESA Workshop on Tracking, Telemetry, and Command System for Space Applications, pp.177-183, 2001.

[6] J.B. Berner, J.M. Layland, P.W. Kinman, and J.R. Smith, "Regenerative Pseudo-Noise Ranging for Deep Space Applications", JPL TMO Progress Report, 42-137, pp.1-18, May 1999.

[7] S. Ohashi, K. Sagawa, A. Yamada, M. Sugiura, M. Miura, T. Atarashiya, Z. Yamamoto, and H. Hirosawa, "S-and X-Band Telemetry, tracking and Command System for Scientific Satellites", NEC R&D, vol.42, No.2, pp.225-229, Apr. 2001.

JAXA Research and Development Report
(JAXA-RR-04-005E)

Date of Issue : Oct 29, 2004

Edited and Published by :
Japan Aerospace Exploration Agency
7-44-1 Jindaiji-higashimachi, Chofu-shi,
Tokyo 182-8522 Japan

Printed by :
FUJIPLANS Co., Ltd.
3-8-17 Nishiki-cho, Tachikawa-shi, Tokyo 190-0022 Japan

Japan Aerospace Exploration Agency